Title: **Zoledronic acid renders human M1 and M2 macrophages susceptible to Vδ2^{+} γδ T cell cytotoxicity in a perforin dependent manner**

Authors: Daniel W Fowler, John Copier, Angus G Dalgleish and Mark D Bodman-Smith

Affiliation: Institute for Infection and Immunity
St. George's University of London
London
UK

Correspondence: Dr Daniel William Fowler
Institute for Infection and Immunity
St. George's University of London
Cranmer Terrace
Tooting
London
SW17 0RE
UK
dfowler@sgul.ac.uk

Abstract

Vδ2$^+$ T cells are a subpopulation of γδ T cells in humans that are cytotoxic towards cells which accumulate isopentenyl pyrophosphate. The nitrogen-containing bisphosphonate, zoledronic acid (ZA), can induce tumour cell lines to accumulate isopentenyl pyrophosphate, thus rendering them more susceptible to Vδ2$^+$ T cell cytotoxicity. However, little is known about whether ZA renders other, non-malignant cell types susceptible. In this study we focussed on macrophages (Mϕs), as these cells have been shown to take up ZA. We differentiated peripheral blood monocytes from healthy donors into Mϕs, and then treated them with IFN-γ or IL-4 to generate M1 and M2 Mϕs, respectively. We characterised these Mϕs based on their phenotype and cytokine production, and then tested whether ZA rendered them susceptible to Vδ2$^+$ T cell cytotoxicity. Consistent with the literature, IFN-γ-treated Mϕs expressed higher levels of the M1 markers CD64 and IL-12p70; whereas, IL-4-treated Mϕs expressed higher levels of the M2 markers CD206 and chemokine (C-C motif) ligand 18. When treated with ZA, both M1 and M2 Mϕs became susceptible to Vδ2$^+$ T cell cytotoxicity. Vδ2$^+$ T cells expressed perforin and degranulated in response to ZA-treated Mϕs as shown by mobilisation of CD107a and CD107b to the cell surface. Furthermore, cytotoxicity towards ZA-treated Mϕs was sensitive—at least in part—to the perforin inhibitor concanamycin A. These findings suggest that ZA can render M1 and M2 Mϕs susceptible to Vδ2$^+$ T cell cytotoxicity in a perforin dependent manner, which has important implications regarding the use of ZA in cancer immunotherapy.

Key words

γδ T cell; Vδ2^{+} T cell; macrophage; zoledronic acid; cytotoxicity.

Précis

This study identifies a novel effect of zoledronic acid on Mϕs and provides a potential mechanism of action that may help the future development of this drug in cancer immunotherapy.

Abbreviations

CCL	=	chemokine (C-C motif) ligand
CFSE	=	carboxyfluorescein succinimidyl ester
CMA	=	concanamycin A
FSC	=	forward scatter
G	=	gate
IPP	=	isopentenyl pyrophosphate
LSD	=	least significant difference
Mϕ	=	macrophage
MFI	=	mean (arithmetic) fluorescence intensity
NBP	=	nitrogen-containing bisphosphonate
SD	=	standard deviation
SSC	=	side scatter
TAM	=	tumour-associated macrophage
ZA	=	zoledronic acid

Introduction

Human peripheral blood contains a subpopulation of γδ T cells that express TCRs composed of Vγ9 and Vδ2 subunits. These cells—referred to here as $V\delta2^{+}$ T cells—typically represent 0.5–5 percent of peripheral blood T cells, and exert potent cytotoxicity against their target cells.

$V\delta2^{+}$ T cells detect intermediates of isoprenoid biosynthesis, namely isopentenyl pyrophosphate (IPP) and (E)-4-hydroxy-3-methyl-but-2-enyl pyrophosphate. IPP is generated by the endogenous mevalonate pathway as well as the exogenous 1-deoxy-D-xylulose-5-phosphate pathway; whereas, (E)-4-hydroxy-3-methyl-but-2-enyl pyrophosphate is generated by the 1-deoxy-D-xylulose-5-phosphate pathway only [1]. The mevalonate pathway is often dysregulated in malignant and infected cells, resulting in accumulation of IPP and increased susceptibility to $V\delta2^{+}$ T cell cytotoxicity [2, 3]. Moreover, certain cells accumulate IPP when exposed to the nitrogen-containing bisphosphonate (NBP), zoledronic acid (ZA) [4], a synthetic drug that inhibits an enzyme of the mevalonate pathway called farnesyl pyrophosphate synthase [5]. Although the precise mechanism of IPP and (E)-4-hydroxy-3-methyl-but-2-enyl pyrophosphate recognition by $V\delta2^{+}$ T cells has yet to be determined, evidence suggests that it is TCR-dependent and involves butyrophilin 3A1 [6].

ZA is typically used to treat complications associated with excessive bone resorption in diseases such as osteoporosis, Paget's disease and metastatic bone disease [7]. In terms of its mode of action, ZA binds to bone and disrupts the activity of bone remodelling cells called osteoclasts [8]. ZA also has potential as an immunotherapy for cancer, the proof of concept for which has already been demonstrated in clinical trials [9-11]. Although in cancer its mode of action is poorly understood, experiments *in vitro* have shown that tumour cell lines from a broad range of haematological and solid malignancies become more susceptible to $V\delta2^{+}$ T cell cytotoxicity when exposed to ZA, suggesting a role for $V\delta2^{+}$ T cells [12-14]. However, the capacity for ZA to induce susceptibility in other, non-malignant cell types is poorly characterised, and could provide insight that helps to better understand the effects of this drug and improve its clinical application. In this study we have focussed on macrophages (denoted here as Mϕs) because these cells have been shown recently to take up NBPs *in vivo* [15] and are implicated in the progression of cancer [16].

Mϕs are tissue-resident phagocytic cells that play a critical role in tissue repair as well as immunity against pathogenic infection and malignant transformation [17]. Mϕs display functional plasticity that is intricately linked to their surrounding microenvironment [18]. Researchers have categorised the different functional states of Mϕs according to their capacity to either promote inflammation or suppress it. At one end of the spectrum are pro-inflammatory Mϕs, also referred to as M1 or classically activated Mϕs, and at the other end are anti-inflammatory Mϕs, also known as M2 or alternatively activated Mϕs [19]. IFN-γ and IL-4 have been identified as key drivers of these opposing M1 and M2 phenotypes, respectively [19].

As part of our ongoing studies into how ZA stimulates anti-tumour responses in $V\delta2^+$ T cells, we identified a previously unexplored effect involving $V\delta2^+$ T cell targeting of myeloid cells. Recently, we showed that ZA can render peripheral blood monocytes susceptible to $V\delta2^+$ T cell cytotoxicity *in vitro* [20]. In a subsequent study by Junankar *et al*, tumour-associated Mϕs (TAMs) in breast cancer were identified as important targets for NBPs *in vivo* [15]. Therefore, we further explored the concept of $V\delta2^+$ T cell targeting of myeloid cells, and found that ZA can render M1 and M2 Mϕs susceptible to $V\delta2^+$ T cell cytotoxicity. Furthermore, we found that $V\delta2^+$ T cell cytotoxicity towards ZA-treated Mϕs was dependent—at least in part—on perforin. This novel insight into the interplay between $V\delta2^+$ T cells and Mϕs has important implications regarding the use of ZA in cancer immunotherapy.

Materials and Methods

PBMC isolation

Anonymised leukocyte cones from healthy donors were obtained from the National Health Service blood transfusion unit at St. George's Hospital, London. PBMCs were isolated by density adjusted centrifugation using Histopaque-1077 (Sigma-Aldrich). RBCs were lysed with ammonium chloride solution and platelets removed by slow-speed centrifugation. PBMCs were resuspended at 2×10^7cells/ml of freezing medium (45% RPMI-1640, 45% FBS and 10% DMSO; all from Sigma-Aldrich) and frozen at −80°C in Mr Frosty freezing containers (Thermo Scientific) prior to transferring them to liquid nitrogen.

Cell culture

All cell culture was carried out in a humidified incubator at 37°C with 5% CO_2. To generate Mϕs, monocytes were isolated from PBMCs using CD14 microbeads according to the manufacturer's instructions (Miltenyi Biotec). Monocytes were resuspended in serum-free medium (RPMI-1640 containing 2mM L-glutamine, 100units/ml penicillin and 100μg/ml streptomycin; all from Sigma-Aldrich) at a density of 3.8×10^5 cells/ml, and 200μls, 2mls or 5mls of cell suspension added per well of 96-well, 12-well or 6-well tissue culture plates, respectively (Thermo Scientific). Monocytes were cultured for 2 hours, after which time the majority of cells were adherent to the tissue culture plate. This process is known to activate monocytes and initiate the macrophage colony-stimulating factor production required for Mϕ differentiation [21]. The adherent monocytes were then cultured for 10 days in complete medium (RPMI-1640 containing 10% FBS, 2mM L-glutamine, 100units/ml penicillin and 100μg/ml streptomycin), after which time the monocytes had differentiated into Mϕs, as indicated by the morphological changes and plastic adherence observed using light microscopy. M1 and M2 Mϕs were generated by adding 25ng/ml of recombinant human IFN-γ or IL-4 (R and D Systems), respectively, on day 7. Mϕs that had not been treated with IFN-γ or IL-4 (designated M0s) were used as controls throughout. 10μM ZA (Sigma-Aldrich) was added to the Mϕs on day 9. To generate pure populations of $V\delta2^+$ T cells, PBMCs were resuspended at 2×10^6 cells/ml of complete medium containing 1μM ZA and 5ng/ml recombinant human IL-2 (R and D Systems), and 250μls of cell suspension added per well of 96-well round-bottomed tissue culture plates (Thermo Scientific). The cells were cultured for 9 days and fed every 2–3 days with fresh medium containing 5ng/ml IL-2. Dead cells and non-γδ T cells were depleted sequentially using dead cell removal kits and TCRγδ negative isolation kits according to the manufacturer's instructions (Miltenyi Biotec). Purity of Vδ2$^+$CD3$^+$ cells was assessed by flow cytometry using PE-conjugated mouse anti-human Vδ2 (clone 123R3; Miltenyi Biotec) and PerCP-conjugated mouse anti-human CD3 (clone SK7; Biolegend) or FITC-conjugated mouse anti-human CD3 (clone HIT3a; Becton Dickinson). For one donor, a high percentage of Vδ1$^+$CD3$^+$ cells was detected post isolation, and so Vδ1$^+$ cells were depleted using allophycocyanin-conjugated recombinant human anti-Vδ1 (clone REA173; Miltenyi Biotec) and anti-allophycocyanin microbeads according the manufacturer's instructions (Miltenyi Biotec; supplementary Fig. 1). We speculate that this donor's PBMCs had a particularly high percentage of Vδ1$^+$ T cells prior to ZA and IL-2 stimulation and/or their Vδ1$^+$ T cells underwent bystander expansion in response to ZA and IL-2.

Flow cytometry

Day 10 Mϕs in 6-well tissue culture plates were washed twice in PBS (Sigma-Aldrich) and cultured for 15 minutes in PBS containing 0.25% trypsin (Life Technologies) and 2mM EDTA (Sigma-Aldrich). Cells were detached by repeated pipetting and then washed in complete medium to deactivate the trypsin. Mϕs were resuspended in flow cytometry buffer (PBS with 1% BSA and 0.09% sodium azide; all from Sigma-Aldrich) containing either FITC-conjugated mouse anti-human CD64 (clone 10.1; Becton Dickinson) or PE-conjugated mouse anti-human CD206 (clone 19.2; Becton Dickinson). Matched isotype controls were used to determine the amount of background expression. After 10 minutes at room temperature, cells were washed in flow cytometry buffer and fixed in CellFIX (Becton Dickinson). Perforin expression in Vδ2$^+$ T cells was assessed in PBMCs cultured with ZA and IL-2 for 0, 1 and 9 days as described in the *cell culture* section. Cells were resuspended in flow cytometry buffer containing PE-conjugated mouse anti-human Vδ2 (clone 123R3; Miltenyi Biotec) and PerCP-conjugated mouse anti-human CD3 (clone SK7; Biolegend). After 10 minutes at room temperature, cells were washed in flow cytometry buffer and simultaneously fixed and permeabilised using Cytofix/Cytoperm (Becton Dickinson) according to manufacturer's instructions. Cells were washed and resuspended in Perm/Wash buffer (Becton Dickinson), and then labelled with FITC-conjugated mouse anti-human perforin (clone δG9; Becton Dickinson) or matched isotype controls. After 10 minutes at room temperature, cells were washed in Perm/Wash buffer and resuspended in flow cytometry buffer.

Samples were acquired on an LSR II flow cytometer (Becton Dickinson) and analysed using FlowJo software. All comparatively analysed samples were acquired on the same day except for the time course of perforin expression where day 0, 1 and 9 samples were acquired on different days. The mean fluorescence intensity (MFI) values stated throughout are arithmetic means.

ELISAs

Day 10 Mϕs in 12-well tissue culture plates were washed twice in PBS and cultured overnight in complete medium (1ml/well) with or without 100ng/ml LPS (*E.coli* 0127:B8; Sigma-Aldrich). The concentration of IL-12p70 and chemokine (C-C motif) ligand (CCL) 18 within cell-free culture supernatants was determined using DuoSet ELISA kits according to the manufacturer's instructions (R and D Systems). Optical densities at 450nm were determined using a microplate reader (Dynex), and concentrations were extrapolated from standard curve data using a four parameter logistic model generated by GraphPad Prism 6 (GraphPad Software). Standard curves were 31.25–2000pg/ml for IL-12p70, and 7.8125–500pg/ml for CCL18.

Carboxyfluorescein succinimidyl ester/Zombie-NIR cytotoxicity assay

Detaching the Mϕs from the tissue culture plates prior to performing the cytotoxicity assays resulted in poor viability; therefore, cytotoxicity was assessed by adding Vδ2$^+$ T cells directly to adherent Mϕs. Day 10 Mϕs in 12-well tissue culture plates were washed twice in PBS and then cultured for 20 minutes in PBS containing 1μM carboxyfluorescein succinimidyl ester (CFSE; Life Technologies). Mϕs were washed three times in complete medium and then cultured overnight with or without 1.52×10^6 autologous Vδ2$^+$ T cells per well in 2mls complete medium to obtain an E:T ratio of 2:1 based on the initial seeding density of monocytes. For some experiments Vδ2$^+$ T cells were pre-treated for 2 hours with or without 100ng/ml concanamycin A (CMA; Abcam) or DMSO, then washed three times in complete medium prior to being cultured with Mϕs. Non-adherent cells were collected and adherent cells detached from the tissue culture plates as described in the *flow cytometry* section. All cells were washed in PBS and then labelled with Zombie-NIR live/dead discrimination dye according to the manufacturer's instructions (Biolegend). Zombie-NIR binds to amine groups on proteins but does not penetrate an intact plasma membrane. Live cells have relatively low expression because only cell surface proteins are available for binding; whereas, dead cells exhibit higher levels of expression because their compromised plasma membrane permits binding to both extracellular and intracellular proteins. After 15 minutes at room temperature, cells were washed in complete medium and fixed in CellFIX. Samples were acquired on an LSR II flow cytometer and analysed using FlowJo software. All comparatively analysed samples were acquired on the same day.

CD107 mobilisation assay

Day 10 Mϕs in 96-well tissue culture plates were washed three times in PBS and then cultured for 5 hours with $1.52×10^5$ autologous $Vδ2^+$ T cells per well in 200μls complete medium to obtain an E:T ratio of 2:1 based on the initial seeding density of monocytes. Allophycocyanin-conjugated mouse anti-human CD107a (clone H4A3; Biolegend) and FITC-conjugated mouse anti-human CD107b (clone H4B4; Biolegend) or matched isotype controls were added directly to the wells at the start of the co-culture along with 1μg/ml of monensin to neutralise intracellular acidity. Cells were then collected and labelled with PE-conjugated mouse anti-human Vδ2 (clone 123R3; Miltenyi Biotec) and PerCP-conjugated mouse anti-human CD3 (clone SK7; Biolegend) as described in the *flow cytometry* section. Samples were acquired on an LSR II flow cytometer and analysed using FlowJo software. All comparatively analysed samples were acquired on the same day.

Statistical analyses

Data in Fig. 1b, 1c, 3b, 3d and 4c was analysed by repeated measures one-way or two-way ANOVA, and comparisons between means carried out using either Tukey's or Sidak's multiple comparison tests (GraphPad Prism 6). *, **, *** and **** were used to indicate p values of <0.05, <0.01, <0.001 and <0.0001, respectively. Gaussian distributions were assumed. Data in Fig. 2b was a three-way (3 × 2 × 2) factorial design repeated six times using cells from six different donors. The three factors were Mϕ type (M0, M1 and M2), ±ZA and ±Vδ2 cells. Data in Fig. 4b was a three-way (3 × 2 × 4) factorial design repeated five times using cells from five different donors. The three factors were Mϕ type (M0, M1 and M2), ±ZA and ±Vδ2 cells (−Vδ2, +Vδ2, +Vδ2[DMSO] and +Vδ2[CMA]). Data in Fig. 2b and 4b was analysed by three-way ANOVA, and comparisons between means carried out using Fisher's Least Significant Difference (LSD; Genstat 18). Assumptions underlying the analysis were checked using the diagnostic plots produced by the software. LSDs at the 5, 1 and 0.1% level are depicted by black intervals, and differences in the means that were greater than this interval were deemed significant to an equivalent p value of <0.05, <0.01 and <0.001, respectively.

Results

ZA did not alter M1 or M2 markers on Mϕs

We differentiated monocytes from the peripheral blood of healthy donors into Mϕs, and treated them with IFN-γ or IL-4 to generate M1 and M2 Mϕs, respectively. We then characterised these Mϕs based on their expression of markers for M1 Mϕs (CD64 and IL-12p70) and M2 Mϕs (CD206 and CCL18) [19, 22]. M1 Mϕs had upregulated expression of CD64; whereas, M2 Mϕs had downregulated CD64 and upregulated CD206 (Fig. 1a and b). Although, statistically, we observed significantly higher levels of CD206 on M1 Mϕs compared with M0 Mϕs in terms of percentage expression, this was not consistent for all donors and not statistically significant in terms of relative MFI (Fig. 1b). Mϕs were then cultured overnight with or without LPS to measure production of IL-12p70 and CCL18, respectively. M1 Mϕs produced more IL-12p70 than M0 and M2 Mϕs; whereas, M2 Mϕs produced more CCL18 than M0 and M1 Mϕs (Fig. 1c). We also tested whether ZA—added for the last 18 hours of culture—had any effect on these markers, and found little or no difference between untreated and ZA-treated Mϕs (Fig. 1). Taken together, this data validates our protocol for generating M1 and M2 Mϕs, and shows that ZA does not alter the M1 and M2 profile of the Mϕs in this system.

ZA rendered M1 and M2 Mϕs susceptible to Vδ2$^+$ T cell cytotoxicity

To obtain sufficient cell numbers for cytotoxicity assays, we stimulated Vδ2$^+$ T cell expansion prior to isolation. Vδ2$^+$ T cell expansion was observed in PBMCs treated with ZA and IL-2 for 9 days, as shown by increased frequencies of Vδ2$^+$CD3$^+$ cells (supplementary Fig. 2). Vδ2$^+$ T cells were purified by sequentially depleting dead cells and non-γδ T cells (mean±standard deviation (SD) for the percentage of Vδ2$^+$CD3$^+$ cells from four donors = 97.2±1.8; supplementary Fig. 2). The percentage of Vδ2$^+$CD3$^+$ cells at day 0 and day 9 pre depletion of dead cells and non-γδ T cells was not assessed routinely; however, purities at day 9 post depletion were assessed for all isolations performed in this study (mean±SD for 14 isolations = 97.7±1.8). We conducted preliminary experiments to determine the optimal E:T ratio and ZA concentration for Vδ2$^+$ T cell-mediated cytotoxicity against ZA-treated Mϕs (supplementary Fig. 3). These experiments showed Vδ2$^+$ T cell cytotoxicity and degranulation against Mϕs treated with 10μM but not 1μM ZA (supplementary Fig. 3). Furthermore, they showed marked killing at the lowest E:T ratio of 2:1 (supplementary Fig. 3). Using the 10μM concentration of ZA and 2:1

E:T ratio, we found that ZA had little or no effect on Mϕ viability in the absence of Vδ2$^+$ T cells, and Vδ2$^+$ T cells did not induce cell death in Mϕs that had not been treated with ZA (Fig. 2a and b). However, there was a marked increase in the amount of cell death in Mϕs that were pre-treated with ZA and then cultured with Vδ2$^+$ T cells (Fig. 2a and b). Although, statistically, Vδ2$^+$ T cell-mediated killing of ZA-treated M1 Mϕs was significantly higher than that of M0 Mϕs, the difference was relatively small and no statistically significant difference was found between M1 and M2 Mϕs (Fig. 2b). These results suggest that Vδ2$^+$ T cells are cytotoxic towards ZA-treated Mϕs irrespective of their M0, M1 and M2 phenotype.

Vδ2$^+$ T cells expressed perforin and degranulated when cultured with ZA-treated Mϕs

Perforin has been shown previously to play a role in γδ T cell cytotoxicity towards tumour cell lines [23, 24]; therefore, we tested whether perforin contributes to Vδ2$^+$ T cell cytotoxicity towards ZA-treated Mϕs. We measured perforin expression by Vδ2$^+$ T cells before, during and after expansion with ZA and IL-2. We found that, although resting Vδ2$^+$ T cells expressed little or no perforin, it was markedly upregulated after one day of culture with ZA and IL-2 (Fig. 3a and b). After 9 days of culture with ZA and IL-2, perforin was downregulated but still expressed by Vδ2$^+$ T cells (Fig. 3a and b). We also measured perforin expression in expanded and isolated Vδ2$^+$ T cells from six donors, and found consistent expression in terms of percentage expression (means±SD = 1.2±0.5 vs. 23.9±7.6 for isotype and test, respectively) and MFI (means±SD = 227.8±15.2 vs. 490.7±104.6 for isotype and test, respectively). To determine if Vδ2$^+$ T cells release perforin when cultured with ZA-treated Mϕs, we measured the mobilisation of lysosomal-associated membrane protein 1 and 2 (i.e. CD107a and CD107b) to the surface of Vδ2$^+$ T cells. CD107a—and to a lesser extent CD107b—was expressed on Vδ2$^+$ T cells that were isolated from PBMCs after 9 days of culture with ZA and IL-2 (Fig. 3c). This may represent residual CD107 expression from the monocyte-dependent degranulation that is induced when PBMCs are exposed to ZA [20]. Vδ2$^+$ T cells upregulated expression of CD107a and CD107b on their cell surface when cultured with ZA-treated Mϕs compared with untreated Mϕs (Fig. 3c and d). This data suggests that Vδ2$^+$ T cells express perforin and degranulate in response to ZA-treated Mϕs, thus implicating a role for perforin in Vδ2$^+$ T cell cytotoxicity towards ZA-treated Mϕs.

Vδ2$^+$ T cell cytotoxicity towards ZA-treated Mϕs was sensitive to concanamycin A

To explore further the potential role of perforin in Vδ2$^+$ T cell cytotoxicity towards ZA-treated Mϕs, we repeated the cytotoxicity assays shown in Fig. 2, but this time pre-treated Vδ2$^+$ T cells with the H^+-ATPase inhibitor CMA. CMA blocks acidification of cytolytic granules, which inhibits perforin-mediated but not Fas ligand-mediated cytotoxicity [25]. We found that pre-treating Vδ2$^+$ T cells with CMA reduced their cytotoxicity towards Mϕs compared with DMSO controls (Fig. 4a and b). We calculated the percentage inhibition for Vδ2$^+$ T cell cytotoxicity towards M0, M1 and M2 Mϕs, and found that Vδ2$^+$ T cell cytotoxicity towards M0 Mϕs was more sensitive to CMA than towards M1 Mϕs (Fig. 4c). To determine whether CMA had an effect on Vδ2$^+$ T cell viability, we applied a gate to CFSE$^-$ cells and calculated the percentage of Zombie-NIR^{low} cells (supplementary Fig. 4a). There was a discernible reduction in Vδ2$^+$ T cell viability in the presence of ZA-treated Mϕs compared with untreated Mϕs; however, there was little or no difference in Vδ2$^+$ T cell viability between the CMA and DMSO treatment groups (supplementary Fig. 4b). These findings suggest that Vδ2$^+$ T cell cytotoxicity towards ZA-treated Mϕs is sensitive—at least in part—to CMA, thus implicating a role for perforin.

Discussion

Vδ2+ T cells in the peripheral blood of humans are regarded as sentinels against infection [26] and malignant transformation [27]. They express the inflammatory homing receptors chemokine (C-C motif) receptor 5 and chemokine (C-X-C motif) receptor 3 [28], and thus infiltrate sites of infection [29] as well as the inflammatory microenvironment of diseased tissues such as tumours [30, 31]. Mϕs are abundant in these tissues, and are likely to interact closely with infiltrating Vδ2+ T cells. We explored the potential interaction between Vδ2+ T cells and Mϕs *in vitro*, and found that ZA can render M1 and M2 Mϕs susceptible to Vδ2+ T cell cytotoxicity in a perforin dependent manner.

ZA has a high affinity for hydroxyapatite [32], and thus binds rapidly to bone following i.v. infusion [33]. Therefore, the Mϕs most likely to be exposed to ZA are those associated with bone and/or the surrounding tissues; for example, the TAMs in bone-related cancers such as osteosarcoma, myeloma and secondary bone metastases associated with cancers of the prostate, lung and breast. Following i.v. infusion, NBPs may also reach tissues other than bone. Intravital imaging in a murine model of breast cancer showed that a fluorescently labelled NBP—given by i.v. injection—leaked from the vasculature of mammary tumours and bound rapidly to granular microcalcifications, which were subsequently engulfed by TAMs [15]. The NBP was not retained in cells other than Mϕs, nor was it retained in B16 tumours, which lack microcalcifications [15]. This study suggests that calcified tissues other than bone can also accumulate NBPs [15]. The lack of cytotoxicity and degranulation at 1μM ZA that was observed in our preliminary optimisation experiments suggests that the Mϕs most likely to be targeted by Vδ2+ T cells following ZA treatment are those associated with calcified tissues where the drug is likely to accumulate, which has important implications regarding the *in vivo* effects of this drug. It is worth noting that uptake of ZA by Mϕs *in vivo* may be markedly different using other methods of delivery such as liposome or nanoparticle encapsulation [34, 35] and localised injection. At the cellular level, experiments conducted *in vitro* suggest that ZA is taken up by myeloid cells such as monocytes, Mϕs and osteoclasts via the process of fluid phase endocytosis [36, 37].

ZA inhibits farnesyl pyrophosphate synthase of the mevalonate pathway, which has been shown *in vitro* to induce apoptosis directly in the murine Mϕ-like cell line J774.2 [38]. A potential mechanism for this effect is accumulation of the pro-apoptotic analogue of ATP, Apppl, which has been reported to accumulate in ZA-treated cells such as osteoclasts and MCF-7 cells [4]. Interestingly, ZA did not affect the viability of Mϕs in our experiments; however, we used relatively short exposure times and did not look at markers of early stage apoptosis such as surface expression of phosphatidyl serine. Inhibition of farnesyl pyrophosphate synthase may also modulate the differentiation and function of Mϕs. For example, when monocyte-derived M2 Mϕs were differentiated in the presence of ZA, they had reduced expression of CD206 and IL-10, and an impaired capacity to promote angiogenesis and tumour cell invasion [39]. ZA also inhibited tumour growth in a murine model of cervical cancer, which correlated with reduced angiogenesis and decreased production of matrix metallopeptidase 9 by Mϕs proximal to and associated with tumours [40]. Furthermore, ZA reduced the onset and growth of tumours in a murine model of breast cancer, which correlated with reduced vascularisation of the tumour, reduced numbers of TAMs, and repolarisation of TAMs from an M2 to M1 phenotype [41]. Taken together, these studies suggest that ZA can modulate the differentiation of Mϕs towards an M1 phenotype. To the best of our knowledge, $V\delta2^+$ T cell targeting of ZA-treated M1 and M2 Mϕs—as suggested by our data—is previously unreported and broadens our understanding of the effects of ZA on Mϕs. Importantly, mice do not develop the $V\delta2^+$ T cell subset that responds to ZA-induced accumulation of IPP because they lack the gene for butyrophilin 3A1 [42], thus highlighting the importance of using human cells for this study.

Our data suggests that ZA has the potential to kill M1 and M2 Mϕs indirectly within tissues that are exposed to the drug and infiltrated by $V\delta2^+$ T cells. Tumours contain an abundant population of Mϕs, which typically express M2 markers and correlate with a poor prognosis [43]. In breast cancer, CCL18 production by TAMs promotes angiogenesis and thus supports tumour growth and dissemination [44]. Furthermore, M2 Mϕs in the bone marrow of multiple myeloma patients have been shown to protect malignant cells from chemotherapy-induced apoptosis [45, 46]. In contrast, osteosarcomas can contain relatively high percentages of M1 Mϕs, which are associated with reduced metastases and improved survival [47]. The potential for ZA to render Mϕs susceptible to $V\delta2^+$ T cells may be beneficial or detrimental depending on which type of Mϕs are present in the tumour. For example, it may be beneficial in patients with breast cancer or myeloma and could explain the promising responses to ZA reported for clinical trials in these cancer types [48, 49]; whereas, it may be counterproductive in osteosarcoma.

It is important to note that our study has focussed on the killing capacity of activated Vδ2$^+$ T cells. Although it would be interesting to compare the cytotoxicity of resting and activated Vδ2$^+$ T cells, the relatively low frequency of Vδ2$^+$ T cells in peripheral blood meant that we were unable to isolate the number of resting Vδ2$^+$ T cells required to perform the cytotoxicity assays used in this study. Whether or not i.v. infusion of ZA—combined with i.v. or s.c. IL-2—can activate peripheral blood Vδ2$^+$ T cells *in vivo* is a point of contention. Current hypotheses state that peripheral blood monocytes take up ZA following i.v. infusion and subsequently activate Vδ2$^+$ T cells [37]; indeed, proliferation and/or differentiation of peripheral blood Vδ2$^+$ T cells has been reported in some patients receiving ZA and IL-2 [9-11]. However, Vδ2$^+$ T cell responses were not observed in all patients [50], and it is unclear whether this is due to lack of activation or detection. Importantly, Vδ2$^+$ T cells that are pre-activated may be more cytotoxic than resting, and thus ZA-induced targeting of Mϕs by Vδ2$^+$ T cells *in vivo* may be suboptimal in patients for which ZA and IL-2 treatment fails to activate their circulating Vδ2$^+$ T cells, thus highlighting the importance of effective Vδ2$^+$ T cell priming in the periphery.

In our study, Vδ2$^+$ T cell cytotoxicity towards M0, M1 and M2 Mϕs was sensitive—at least in part—to the perforin inhibitor CMA, thus implicating a role for perforin [25]. Interestingly, CMA did not inhibit cytotoxicity completely, and the degree of inhibition varied between the different types of Mϕ; specifically, Vδ2$^+$ T cell cytotoxicity towards M0 Mϕs was more sensitive to CMA than towards M1 Mϕs. If, in our assays, CMA blocked perforin completely, our data would suggest that other mechanisms of cell-mediated cytotoxicity are involved, and that the contribution of perforin versus other mechanisms of cytotoxicity varies between the different types of Mϕ. Indeed, Vδ2$^+$ T cells have been shown to kill target cells through the expression of Fas ligand and TRAIL [51]. However, if perforin blockade was incomplete, the variation in sensitivity to CMA that was observed between the different types of Mϕ could also be attributed to differences in their susceptibility to perforin-mediated killing under conditions of suboptimal perforin activity. Nonetheless, our data suggests that perforin plays a role, which provides a useful mechanistic marker for exploring this concept *in vivo*.

In conclusion, this study sheds light on a potential interaction between Vδ2^{+} T cells and Mϕs following ZA treatment, and suggests a mechanism of action for this drug that may help its future development in cancer immunotherapy.

Acknowledgments

The authors would like to thank the Institute for Cancer Vaccines and Immunotherapy (registered charity number 1080343) for funding this research.

The authors would like to thank Dr David Lovell, Reader in Medical Statistics at St. George's University of London, for his advice and expertise in performing the statistical analyses using ANOVA for the three-way factorial design.

Conflict of interest

The authors declare that they have no conflict of interest.

Figure legends

Figure 1: Characterisation of M1 and M2 Mϕs treated with or without ZA. **(a)** and **(b)** Flow cytometry was used to measure the expression of CD64 and CD206 on M0, M1 and M2 Mϕs treated with (*orange*) or without (*blue*) ZA for the last 18 hours of culture. **(a)** Representative flow cytometry plots from one of six donors (−ZA). Dead cells and debris were excluded based on forward scatter (FSC) and side scatter (SSC) using gate (G) 1. Unfilled overlays = test, filled overlays = isotype. Numbers on the plots are percentage of cells within the marker. **(b)** Individual data points and means for six donors. Test MFIs for the total G1 population were divided by isotype controls to obtain relative MFIs. **(c)** M0, M1 and M2 Mϕs treated with (*orange*) or without (*blue*) ZA for the last 18 hours of culture were cultured overnight in fresh medium with or without 100ng/ml LPS. The concentration of IL-12p70 and CCL18 in culture supernatants was measured using ELISAs. Data for IL-12p70 is in the presence of LPS; whereas, data for CCL18 is in the absence of LPS. Individual data points and means for six donors are shown. For **(b)** and **(c)**, data was analysed by repeated measures two-way ANOVA, and comparisons between means carried out using Tukey's multiple comparison tests. *** and **** indicate p values of <0.001 and <0.0001, respectively. Statistical differences for comparisons within the +ZA (*orange*) data sets are not shown.

Figure 2: Vδ2$^+$ T cell cytotoxicity towards ZA-treated M1 and M2 Mϕs. M0, M1 and M2 Mϕs treated with or without ZA for the last 18 hours of culture were labelled with CFSE and cultured overnight with or without autologous Vδ2$^+$ T cells. Flow cytometry was then used to measure Zombie-NIR expression. **(a)** Representative flow cytometry contour plots from one of six donors showing the gating strategy used to determine Zombie-NIR expression in M0 Mϕs. Mϕs were gated based on FSC and SSC using G1. CFSE$^+$ cells within G1 were gated using G2. The percentage of Zombie-NIR^{high} cells (i.e. dead cells) within G1+G2 was then determined using G3. Numbers on the contour plots are percentages of cells within G3. **(b)** Individual data points and means for six donors. Data was analysed by three-way ANOVA, and comparisons between means carried out using Fisher's LSD tests. The 5, 1 and 0.1% LSDs are depicted by the black intervals.

<u>Figure 3: Expression of perforin and mobilisation of CD107a and CD107b in Vδ2$^+$ T cells.</u> (a) and **(b)** Flow cytometry was used to measure the expression of perforin by Vδ2$^+$ T cells in PBMCs cultured with ZA and IL-2 for 0, 1 and 9 days. **(a)** Representative flow cytometry plots from one of three donors showing perforin expression in Vδ2$^+$ T cells. Lymphocytes were gated based on FSC and SSC using G1. Note that G1 was extended at day 9 to incorporate blast cells. Vδ2$^+$CD3$^+$ cells within G1 were gated using G2. Percentage expression and MFI of perforin within G1+G2 was then assessed. Unfilled overlays = test, filled overlays = isotype. Numbers on the histogram plots are percentage of cells within the marker. **(b)** Means±SD for three donors. Test MFIs for the total G1+G2 population were divided by the isotype controls to obtain relative MFIs. Data was analysed by repeated measures one-way ANOVA, and comparisons between means carried out using Tukey's multiple comparison tests. **(c)** and **(d)** Vδ2$^+$ T cells were cultured with or without autologous M0, M1 or M2 Mϕs that had been treated with or without ZA for the last 18 hours of culture. Flow cytometry was used to measure the expression of CD107a and CD107b by Vδ2$^+$ T cells. **(c)** Representative flow cytometry contour plots from one of three donors showing CD107a and CD107b expression on gated Vδ2$^+$CD3$^+$ cells. Lymphocytes were gated based on FSC and SSC using G1. Vδ2$^+$CD3$^+$ cells within G1 were gated using G2. Percentage expression of CD107a and CD107b within G1+G2 was then assessed. Quadrants were set against the Vδ2 alone controls, and separate quadrants were generated for isotype and test. Numbers are percentages of cells contained within the upper right quadrants. **(d)** Individual data points and means for three donors. Data was analysed by repeated measures two-way ANOVA, and comparisons between means carried out using Sidak's multiple comparison tests. For **(b)** and **(d)**, *, **, *** and **** indicate p values of <0.05, <0.01, <0.001 and <0.0001, respectively.

<u>Figure 4: The effect of concanamycin A on Vδ2$^+$ T cell cytotoxicity towards ZA-treated Mϕs.</u> M0, M1 and M2 Mϕs treated with or without ZA for the last 18 hours of culture were labelled with CFSE and then cultured overnight with or without autologous Vδ2$^+$ T cells that had been pre-treated for two hours with or without CMA (100ng/ml) or DMSO. Flow cytometry was then used to measure Zombie-NIR expression. **(a)** Representative flow cytometry contour plots for M0 Mϕs from one of five donors. The percentage of Zombie-NIR^{high} cells (i.e. dead cells) within CFSE$^+$ Mϕs was determined using the G1+G2+G3 gating strategy described in Fig. 2. Numbers on the plots are percentages of cells within G3. **(b)** Individual data points and means for five donors. Data was analysed by three-way ANOVA, and comparisons between means carried out using Fisher's LSD tests. The 0.1% LSD is depicted by the black interval. **(c)** Data in **(b)** was expressed as percentage inhibition. Within the +ZA data sets, the percentage of dead Mϕs in the absence of $V\delta 2^{+}$ T cells (i.e. background cell death) was subtracted from that induced by the DMSO- and CMA-treated $V\delta 2^{+}$ T cells. The corrected values for Mϕ cell death induced by CMA-treated $V\delta 2^{+}$ T cells were then expressed as a percentage of the corrected values for Mϕ cell death induced by DMSO-treated $V\delta 2^{+}$ T cells. These values were then converted to percentage inhibition by subtracting them from 100%. Data was analysed by repeated measures one-way ANOVA, and comparisons between means carried out using Tukey's multiple comparison tests. ** indicates a p value <0.01.

1. Morita CT, Jin C, Sarikonda G, Wang H (2007) Nonpeptide antigens, presentation mechanisms, and immunological memory of human Vgamma2Vdelta2 T cells: discriminating friend from foe through the recognition of prenyl pyrophosphate antigens. Immunol Rev 215: 59-76.

2. Gober HJ, Kistowska M, Angman L, Jeno P, Mori L, De Libero G (2003) Human T cell receptor gammadelta cells recognize endogenous mevalonate metabolites in tumor cells. J Exp Med 197: 163-168.

3. Kistowska M, Rossy E, Sansano S, Gober HJ, Landmann R, Mori L, De Libero G (2008) Dysregulation of the host mevalonate pathway during early bacterial infection activates human TCR gamma delta cells. Eur J Immunol 38: 2200-2209.

4. Raikkonen J, Crockett JC, Rogers MJ, Monkkonen H, Auriola S, Monkkonen J (2009) Zoledronic acid induces formation of a pro-apoptotic ATP analogue and isopentenyl pyrophosphate in osteoclasts in vivo and in MCF-7 cells in vitro. Br J Pharmacol 157: 427-435.

5. Kavanagh KL, Guo K, Dunford JE, Wu X, Knapp S, Ebetino FH, Rogers MJ, Russell RG, Oppermann U (2006) The molecular mechanism of nitrogen-containing bisphosphonates as antiosteoporosis drugs. Proc Natl Acad Sci U S A 103: 7829-7834.

6. Harly C, Guillaume Y, Nedellec S, Peigne CM, Monkkonen H, Monkkonen J, Li J, Kuball J, Adams EJ, Netzer S, Dechanet-Merville J, Leger A, Herrmann T, Breathnach R, Olive D, Bonneville M, Scotet E (2012) Key implication of CD277/butyrophilin-3 (BTN3A) in cellular stress sensing by a major human gammadelta T-cell subset. Blood 120: 2269-2279.

7. Lipton A (2005) New therapeutic agents for the treatment of bone diseases. Expert Opin Biol Ther 5: 817-832.

8. Benford HL, McGowan NW, Helfrich MH, Nuttall ME, Rogers MJ (2001) Visualization of bisphosphonate-induced caspase-3 activity in apoptotic osteoclasts in vitro. Bone 28: 465-473.

9. Dieli F, Vermijlen D, Fulfaro F, Caccamo N, Meraviglia S, Cicero G, Roberts A, Buccheri S, D'Asaro M, Gebbia N, Salerno A, Eberl M, Hayday AC (2007) Targeting human {gamma}delta} T cells with

zoledronate and interleukin-2 for immunotherapy of hormone-refractory prostate cancer. Cancer Res 67: 7450-7457.

10. Meraviglia S, Eberl M, Vermijlen D, Todaro M, Buccheri S, Cicero G, La Mendola C, Guggino G, D'Asaro M, Orlando V, Scarpa F, Roberts A, Caccamo N, Stassi G, Dieli F, Hayday AC (2010) In vivo manipulation of Vgamma9Vdelta2 T cells with zoledronate and low-dose interleukin-2 for immunotherapy of advanced breast cancer patients. Clin Exp Immunol 161: 290-297.

11. Kunzmann V, Smetak M, Kimmel B, Weigang-Koehler K, Goebeler M, Birkmann J, Becker J, Schmidt-Wolf IG, Einsele H, Wilhelm M (2012) Tumor-promoting versus tumor-antagonizing roles of gammadelta T cells in cancer immunotherapy: results from a prospective phase I/II trial. J Immunother 35: 205-213.

12. Wrobel P, Shojaei H, Schittek B, Gieseler F, Wollenberg B, Kalthoff H, Kabelitz D, Wesch D (2007) Lysis of a broad range of epithelial tumour cells by human gamma delta T cells: involvement of NKG2D ligands and T-cell receptor- versus NKG2D-dependent recognition. Scand J Immunol 66: 320-328.

13. Bouet-Toussaint F, Cabillic F, Toutirais O, Le Gallo M, Thomas de la Pintiere C, Daniel P, Genetet N, Meunier B, Dupont-Bierre E, Boudjema K, Catros V (2008) Vgamma9Vdelta2 T cell-mediated recognition of human solid tumors. Potential for immunotherapy of hepatocellular and colorectal carcinomas. Cancer Immunol Immunother 57: 531-539.

14. Saitoh A, Narita M, Watanabe N, Tochiki N, Satoh N, Takizawa J, Furukawa T, Toba K, Aizawa Y, Shinada S, Takahashi M (2008) Anti-tumor cytotoxicity of gammadelta T cells expanded from peripheral blood cells of patients with myeloma and lymphoma. Med Oncol 25: 137-147.

15. Junankar S, Shay G, Jurczyluk J, Ali N, Down J, Pocock N, Parker A, Nguyen A, Sun S, Kashemirov B, McKenna CE, Croucher PI, Swarbrick A, Weilbaecher K, Phan TG, Rogers MJ (2015) Real-time intravital imaging establishes tumor-associated macrophages as the extraskeletal target of bisphosphonate action in cancer. Cancer Discov 5: 35-42.

16. Mills CD, Lenz LL, Harris RA (2016) A Breakthrough: Macrophage-Directed Cancer Immunotherapy. Cancer Res 76: 513-516.

17. Murray PJ and Wynn TA (2011) Protective and pathogenic functions of macrophage subsets. Nat Rev Immunol 11: 723-737.

18. Biswas SK and Mantovani A (2010) Macrophage plasticity and interaction with lymphocyte subsets: cancer as a paradigm. Nat Immunol 11: 889-896.

19. Murray PJ, Allen JE, Biswas SK, Fisher EA, Gilroy DW, Goerdt S, Gordon S, Hamilton JA, Ivashkiv LB, Lawrence T, Locati M, Mantovani A, Martinez FO, Mege JL, Mosser DM, Natoli G, Saeij JP, Schultze JL, Shirey KA, Sica A, et al (2014) Macrophage activation and polarization: nomenclature and experimental guidelines. Immunity 41: 14-20.

20. Fowler DW, Copier J, Dalgleish AG, Bodman-Smith MD (2014) Zoledronic acid causes gammadelta T cells to target monocytes and down-modulate inflammatory homing. Immunology 143: 539-549.

21. Wahl LM, Wahl SM, Smythies LE, Smith PD (2006) Isolation of human monocyte populations. Curr Protoc Immunol. Chapter 7: Unit 7.6A.

22. Ambarus CA, Krausz S, van Eijk M, Hamann J, Radstake TR, Reedquist KA, Tak PP, Baeten DL (2012) Systematic validation of specific phenotypic markers for in vitro polarized human macrophages. J Immunol Methods 375: 196-206.

23. Alexander AA, Maniar A, Cummings JS, Hebbeler AM, Schulze DH, Gastman BR, Pauza CD, Strome SE, Chapoval AI (2008) Isopentenyl pyrophosphate-activated CD56+ {gamma}{delta} T lymphocytes display potent antitumor activity toward human squamous cell carcinoma. Clin Cancer Res 14: 4232-4240.

24. Mattarollo SR, Kenna T, Nieda M, Nicol AJ (2007) Chemotherapy and zoledronate sensitize solid tumour cells to Vgamma9Vdelta2 T cell cytotoxicity. Cancer Immunol Immunother 56: 1285-1297.

25. Kataoka T, Shinohara N, Takayama H, Takaku K, Kondo S, Yonehara S, Nagai K (1996) Concanamycin A, a powerful tool for characterization and estimation of contribution of perforin- and Fas-based lytic pathways in cell-mediated cytotoxicity. J Immunol 156: 3678-3686.

26. Dieli F, Troye-Blomberg M, Farouk SE, Sireci G, Salerno A (2001) Biology of gammadelta T cells in tuberculosis and malaria. Curr Mol Med 1: 437-446.

27. Fowler DW and Bodman-Smith MD (2015) Harnessing the power of Vdelta2 cells in cancer immunotherapy. Clin Exp Immunol 180: 1-10.

28. Glatzel A, Wesch D, Schiemann F, Brandt E, Janssen O, Kabelitz D (2002) Patterns of chemokine receptor expression on peripheral blood gamma delta T lymphocytes: strong expression of CCR5 is a selective feature of V delta 2/V gamma 9 gamma delta T cells. J Immunol 168: 4920-4929.

29. Liuzzi AR, Kift-Morgan A, Lopez-Anton M, Friberg IM, Zhang J, Brook AC, Roberts GW, Donovan KL, Colmont CS, Toleman MA, Bowen T, Johnson DW, Topley N, Moser B, Fraser DJ, Eberl M (2016) Unconventional Human T Cells Accumulate at the Site of Infection in Response to Microbial Ligands and Induce Local Tissue Remodeling. J Immunol 197: 2195-2207.

30. Cordova A, Toia F, La Mendola C, Orlando V, Meraviglia S, Rinaldi G, Todaro M, Cicero G, Zichichi L, Donni PL, Caccamo N, Stassi G, Dieli F, Moschella F (2012) Characterization of human gammadelta T lymphocytes infiltrating primary malignant melanomas. PLoS One 7: e49878.

31. Bank I, Book M, Huszar M, Baram Y, Schnirer I, Brenner H (1993) V delta 2+ gamma delta T lymphocytes are cytotoxic to the MCF 7 breast carcinoma cell line and can be detected among the T cells that infiltrate breast tumors. Clin Immunol Immunopathol 67: 17-24.

32. Lawson MA, Xia Z, Barnett BL, Triffitt JT, Phipps RJ, Dunford JE, Locklin RM, Ebetino FH, Russell RG (2010) Differences between bisphosphonates in binding affinities for hydroxyapatite. J Biomed Mater Res B Appl Biomater 92: 149-155.

33. Kimmel DB (2007) Mechanism of action, pharmacokinetic and pharmacodynamic profile, and clinical applications of nitrogen-containing bisphosphonates. J Dent Res 86: 1022-1033.

34. Marra M, Salzano G, Leonetti C, Porru M, Franco R, Zappavigna S, Liguori G, Botti G, Chieffi P, Lamberti M, Vitale G, Abbruzzese A, La Rotonda MI, De Rosa G, Caraglia M (2012) New self-assembly nanoparticles and stealth liposomes for the delivery of zoledronic acid: a comparative study. Biotechnol Adv 30: 302-309.

35. Schiraldi C, Zappavigna S, D'Agostino A, Porto S, Gaito O, Lusa S, Lamberti M, De Rosa M, De Rosa G, Caraglia M (2014) Nanoparticles for the delivery of zoledronic acid to prostate cancer cells: a comparative analysis through time lapse video-microscopy technique. Cancer Biol Ther 15: 1524-1532.

36. Thompson K, Rogers MJ, Coxon FP, Crockett JC (2006) Cytosolic entry of bisphosphonate drugs requires acidification of vesicles after fluid-phase endocytosis. Mol Pharmacol 69: 1624-1632.

37. Roelofs AJ, Jauhiainen M, Monkkonen H, Rogers MJ, Monkkonen J, Thompson K (2009) Peripheral blood monocytes are responsible for gammadelta T cell activation induced by zoledronic acid through accumulation of IPP/DMAPP. Br J Haematol 144: 245-250.

38. Rogers TL, Wind N, Hughes R, Nutter F, Brown HK, Vasiliadou I, Ottewell PD, Holen I (2013) Macrophages as potential targets for zoledronic acid outside the skeleton-evidence from in vitro and in vivo models. Cell Oncol (Dordr) 36: 505-514.

39. Comito G, Segura CP, Taddei ML, Lanciotti M, Serni S, Morandi A, Chiarugi P, Giannoni E (2017) Zoledronic acid impairs stromal reactivity by inhibiting M2-macrophages polarization and prostate cancer-associated fibroblasts. Oncotarget 8: 118-132.

40. Giraudo E, Inoue M, Hanahan D (2004) An amino-bisphosphonate targets MMP-9-expressing macrophages and angiogenesis to impair cervical carcinogenesis. J Clin Invest 114: 623-633.

41. Coscia M, Quaglino E, Iezzi M, Curcio C, Pantaleoni F, Riganti C, Holen I, Monkkonen H, Boccadoro M, Forni G, Musiani P, Bosia A, Cavallo F, Massaia M (2010) Zoledronic acid repolarizes tumour-associated macrophages and inhibits mammary carcinogenesis by targeting the mevalonate pathway. J Cell Mol Med 14: 2803-2815.

42. Karunakaran MM, Gobel TW, Starick L, Walter L, Herrmann T (2014) Vgamma9 and Vdelta2 T cell antigen receptor genes and butyrophilin 3 (BTN3) emerged with placental mammals and are concomitantly preserved in selected species like alpaca (Vicugna pacos). Immunogenetics 66: 243-254.

43. Schmieder A, Michel J, Schonhaar K, Goerdt S, Schledzewski K (2012) Differentiation and gene expression profile of tumor-associated macrophages. Semin Cancer Biol 22: 289-297.

44. Lin L, Chen YS, Yao YD, Chen JQ, Chen JN, Huang SY, Zeng YJ, Yao HR, Zeng SH, Fu YS, Song EW (2015) CCL18 from tumor-associated macrophages promotes angiogenesis in breast cancer. Oncotarget 6: 34758-34773.

45. Beider K, Bitner H, Leiba M, Gutwein O, Koren-Michowitz M, Ostrovsky O, Abraham M, Wald H, Galun E, Peled A, Nagler A (2014) Multiple myeloma cells recruit tumor-supportive macrophages through the CXCR4/CXCL12 axis and promote their polarization toward the M2 phenotype. Oncotarget 5: 11283-11296.

46. Zheng Y, Cai Z, Wang S, Zhang X, Qian J, Hong S, Li H, Wang M, Yang J, Yi Q (2009) Macrophages are an abundant component of myeloma microenvironment and protect myeloma cells from chemotherapy drug-induced apoptosis. Blood 114: 3625-3628.

47. Buddingh EP, Kuijjer ML, Duim RA, Burger H, Agelopoulos K, Myklebost O, Serra M, Mertens F, Hogendoorn PC, Lankester AC, Cleton-Jansen AM (2011) Tumor-infiltrating macrophages are associated with metastasis suppression in high-grade osteosarcoma: a rationale for treatment with macrophage activating agents. Clin Cancer Res 17: 2110-2119.

48. Aviles A, Neri N, Huerta-Guzman J, Nambo MJ (2013) Randomized clinical trial of zoledronic acid in multiple myeloma patients undergoing high-dose chemotherapy and stem-cell transplantation. Curr Oncol 20: e13-20.

49. Valachis A, Polyzos NP, Coleman RE, Gnant M, Eidtmann H, Brufsky AM, Aft R, Tevaarwerk AJ, Swenson K, Lind P, Mauri D (2013) Adjuvant therapy with zoledronic acid in patients with breast cancer: a systematic review and meta-analysis. Oncologist 18: 353-361.

50. Lang JM, Kaikobad MR, Wallace M, Staab MJ, Horvath DL, Wilding G, Liu G, Eickhoff JC, McNeel DG, Malkovsky M (2011) Pilot trial of interleukin-2 and zoledronic acid to augment gammadelta T cells as treatment for patients with refractory renal cell carcinoma. Cancer Immunol Immunother 60: 1447-1460.

51. Li H, Xiang Z, Feng T, Li J, Liu Y, Fan Y, Lu Q, Yin Z, Yu M, Shen C, Tu W (2013) Human Vgamma9Vdelta2-T cells efficiently kill influenza virus-infected lung alveolar epithelial cells. Cell Mol Immunol 10: 159-164.

Figure 1

Click here to download Figure CII REVISED FIGURE 1.pptx

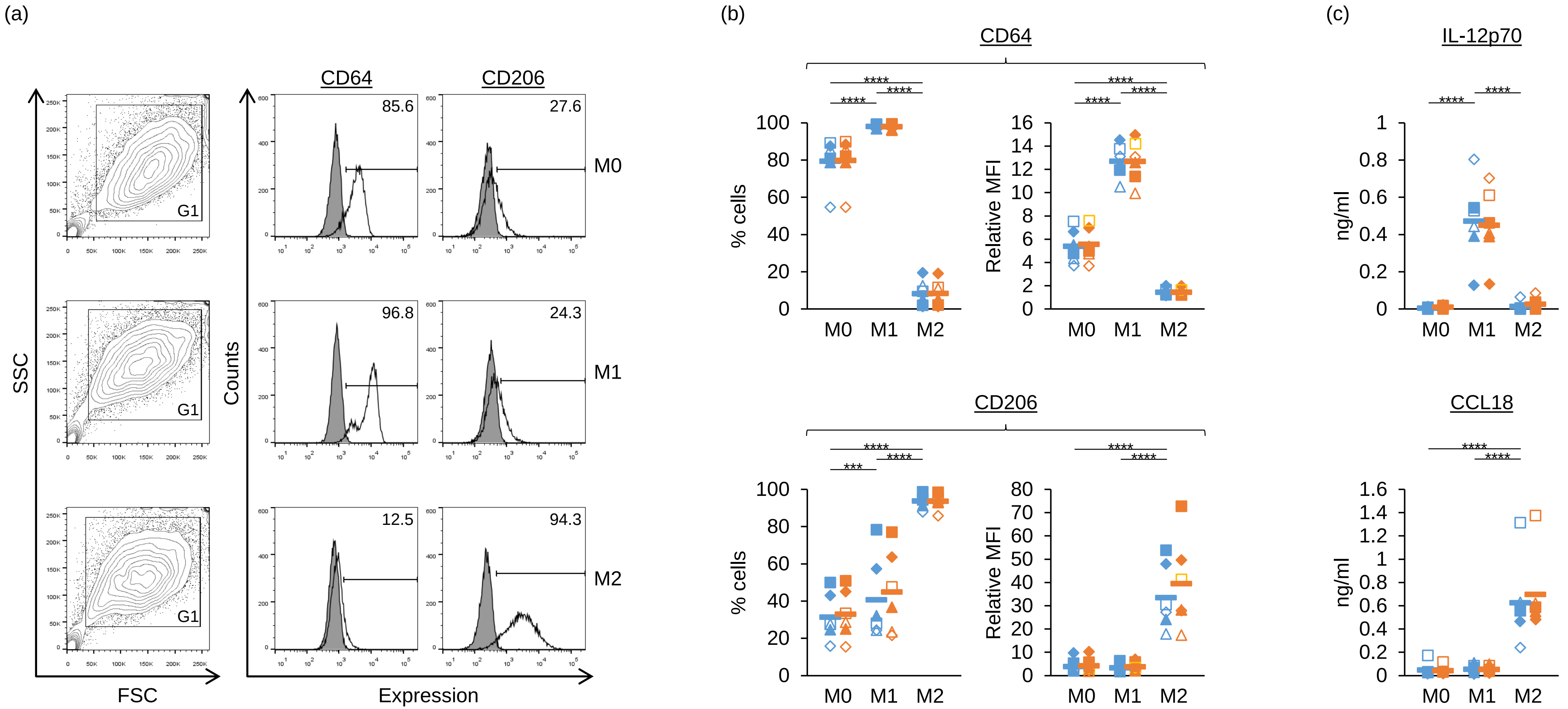

Figure 2

Click here to download Figure CII REVISED FIGURE 2.pptx

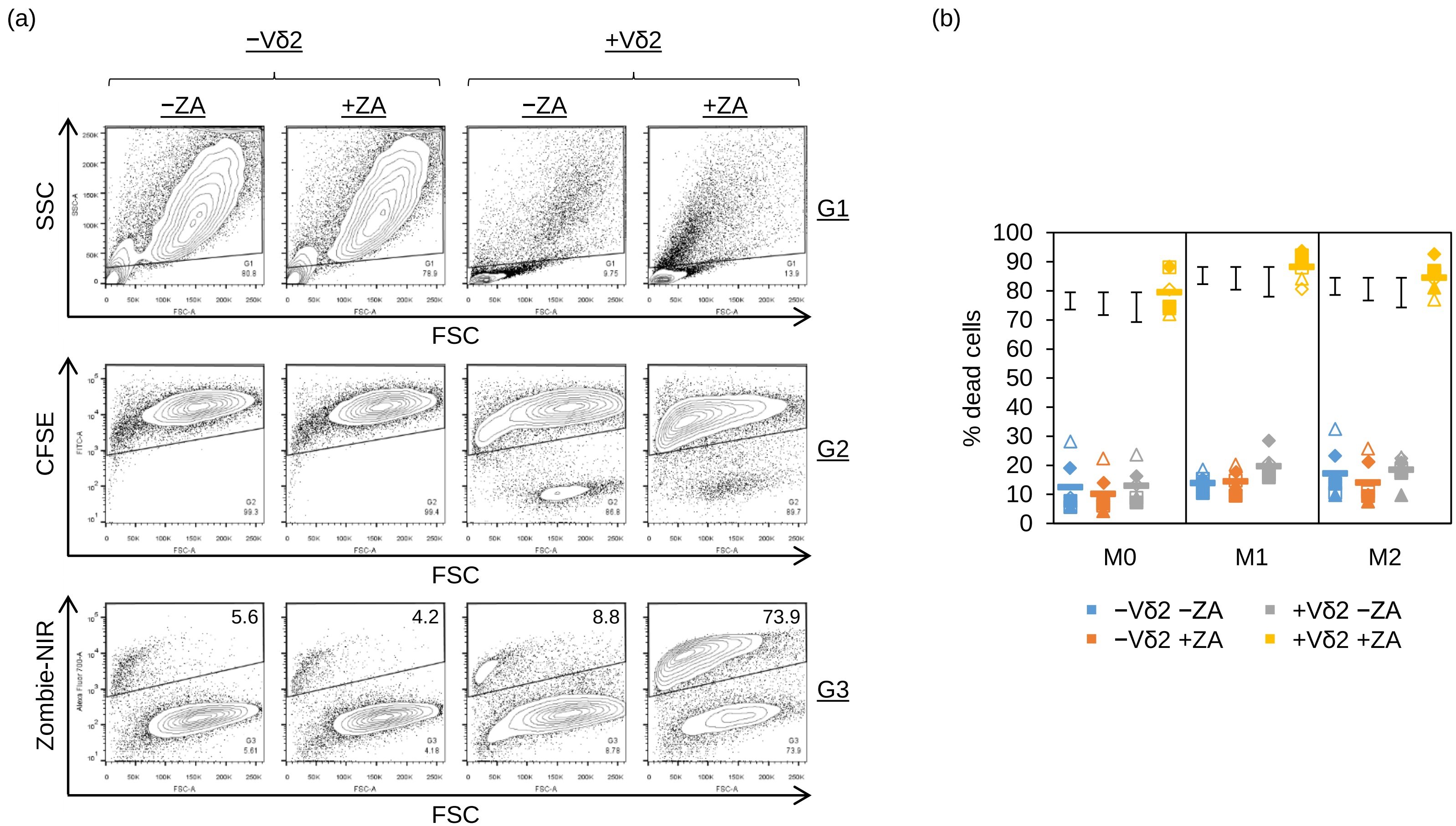

Figure 3

Click here to download Figure CII R2 FIGURE 3.pptx

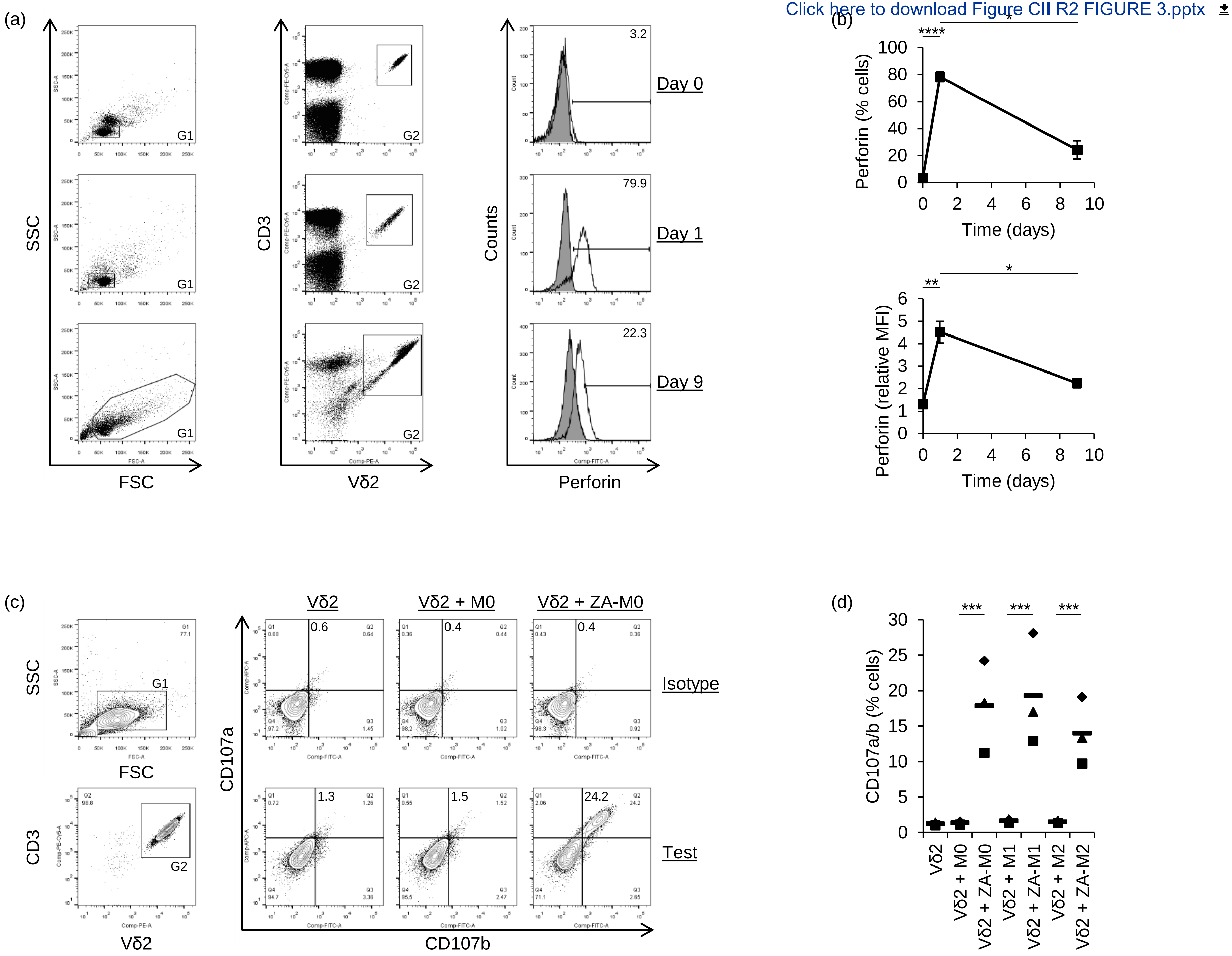

Figure 4

Click here to download Figure CII REVISED FIGURE 4.pptx

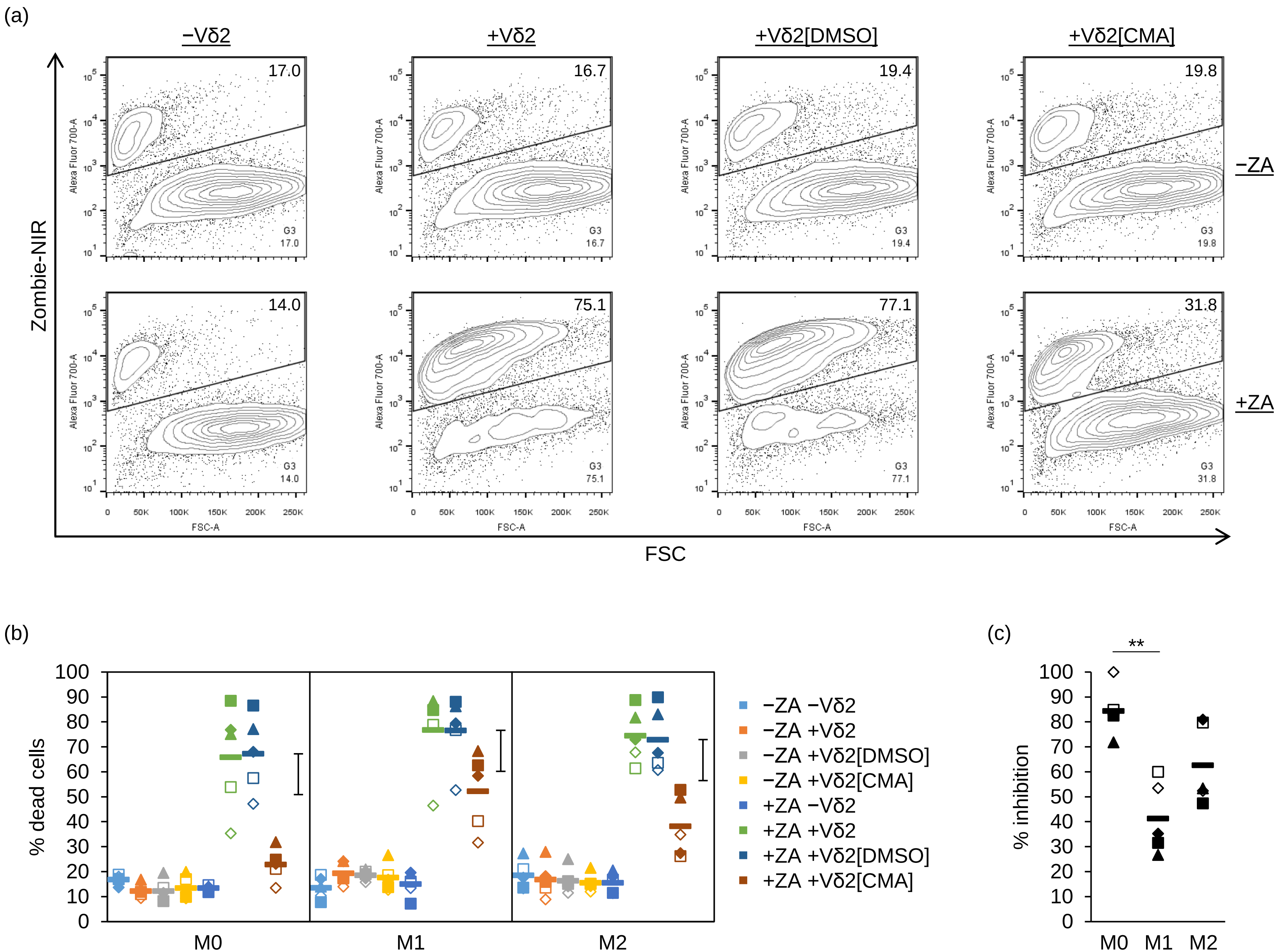

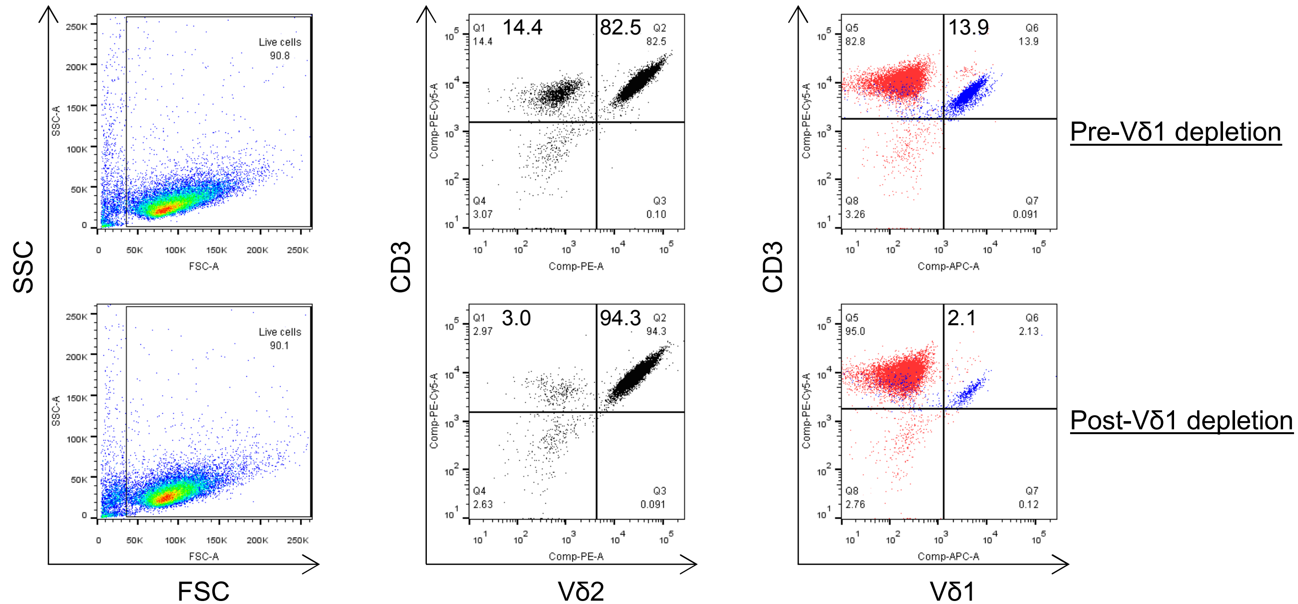

<u>Supplementary Fig. 1: The additional Vδ1⁺ T cell depletion step used to increase the purity of Vδ2⁺ T cells from one of the donors.</u> PBMCs were treated for 9 days with 1μM ZA and 5ng/ml IL-2. Culture medium was replaced with fresh medium containing 5ng/ml IL-2 every 2–3 days. Dead cells, non-γδ T cells and Vδ1^{+} cells were depleted sequentially using MACS. Flow cytometry was used to measure the percentage of Vδ2^{+}CD3^{+} and Vδ1^{+}CD3^{+} cells pre- and post-Vδ1^{+} cell depletion. Flow cytometry plots are from one donor. Dead cells and debris were excluded based on FSC and SSC, and Vδ2, Vδ1 and CD3 expression was assessed on gated cells. Numbers on the dot plots are percentages of cells contained within the quadrants. Vδ2^{-}CD3^{+} cells (i.e. cells in the upper left quadrant of the middle column of dot plots) were coloured blue on the Vδ1 vs. CD3 dot plots on the right hand side.

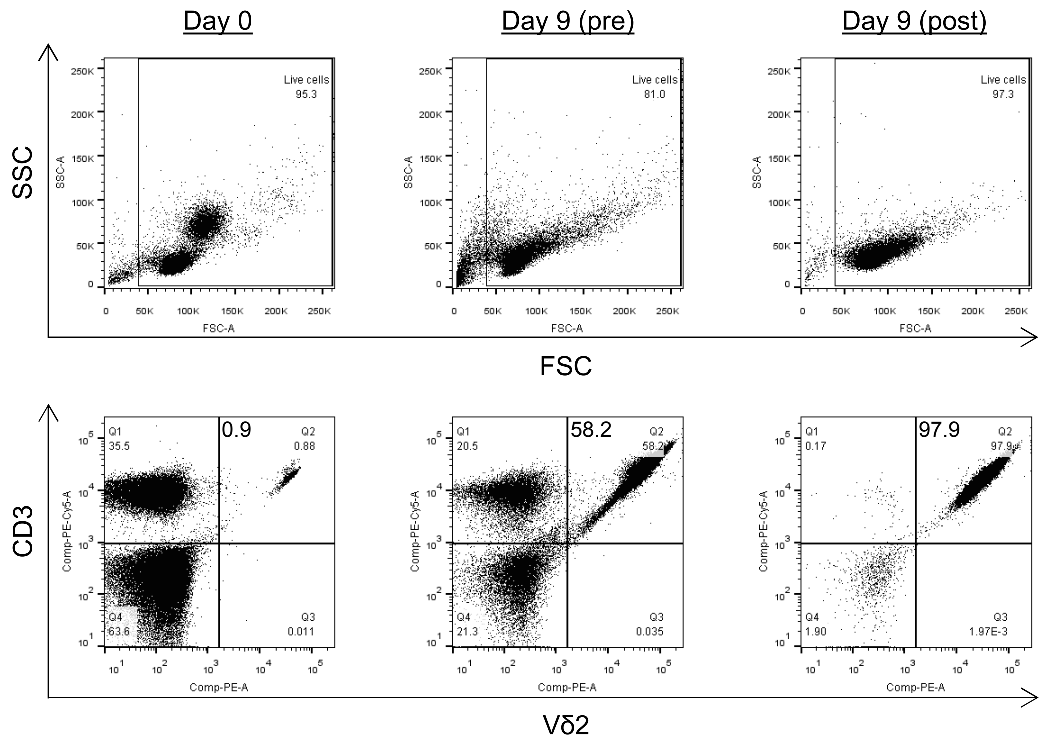

Supplementary Fig. 2: Expansion and isolation of Vδ2⁺ T cells. PBMCs were treated for 9 days with 1μM ZA and 5ng/ml IL-2. Culture medium was replaced with fresh medium containing 5ng/ml IL-2 every 2–3 days. Dead cells and non-γδ T cells were then depleted sequentially using MACS. Flow cytometry was used to measure the percentage of $V\delta2^{+}CD3^{+}$ cells at day 0 and 9 pre and post depletion of dead cells and non-γδ T cells. Representative flow cytometry dot plots from one of four donors are shown. Dead cells and debris were excluded based on FSC and SSC, and Vδ2 and CD3 expression was assessed on gated cells. Numbers on the dot plots are percentages of cells contained within the upper right quadrants.

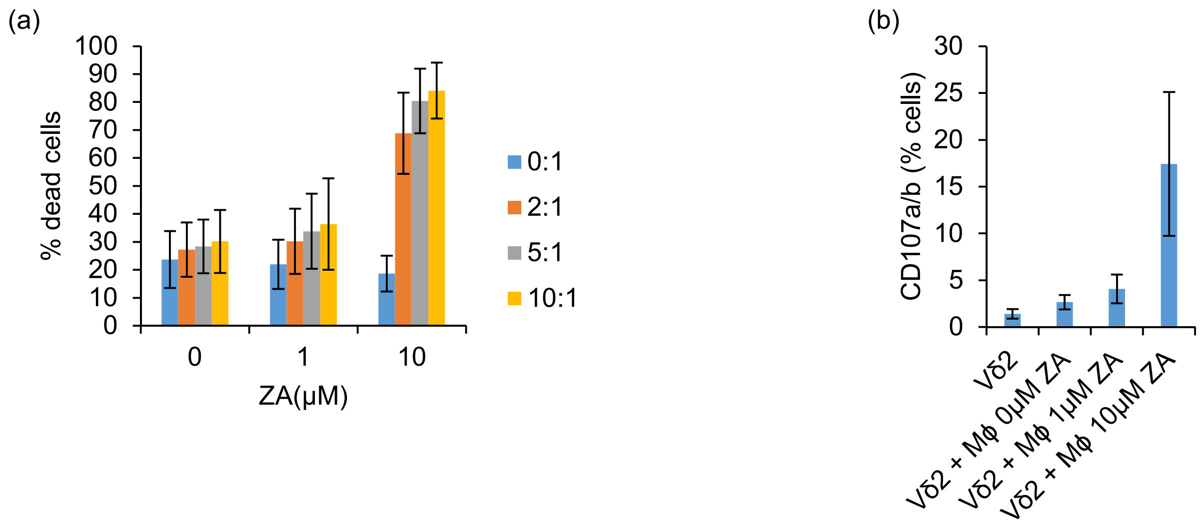

Supplementary Fig. 3: Preliminary optimisation experiments used to determine the concentration of ZA and E:T ratio for cytotoxicity assays. CD14$^+$ cells were cultured for 2 hours in serum-free medium and then cultured for 10 days in 10% FBS medium. 25ng/ml IFN-γ was added for the last 48 hours, and 100ng/ml LPS with or without 1 or 10μM ZA was added for the last 18 hours. **(a)** Day 10 Mϕs were washed twice in PBS and then cultured for 20 minutes in PBS containing 1μM CFSE. CFSE$^+$ Mϕs were washed three times in complete medium and cultured for 5 hours with or without autologous Vδ2$^+$ T cells (generated as described in the materials and methods) at E:T ratios of 2:1, 5:1 and 10:1. Cells were then stained with Zombie-NIR and the percentage of Zombie NIR^{high} cells within CFSE$^+$ cells determined by flow cytometry using the gating strategy described in Fig. 2. **(b)** Day 10 Mϕs were washed three times in complete medium and cultured for 5 hours with or without autologous Vδ2$^+$ T cells (generated as described in the materials and methods) at an E:T ratio of 2:1. Expression of CD107a and CD107b on Vδ2$^+$ T cells was then measured by flow cytometry as described in the materials and methods using the gating strategy described in Fig. 3. For **(a)** and **(b)**, means±SD for three donors are shown and the E:T ratios were based on the number of monocytes seeded at the start of Mϕ differentiation. Results show Vδ2$^+$ T cell-mediated killing of Mϕs at the E:T ratio of 2:1 and the 10μM concentration of ZA.

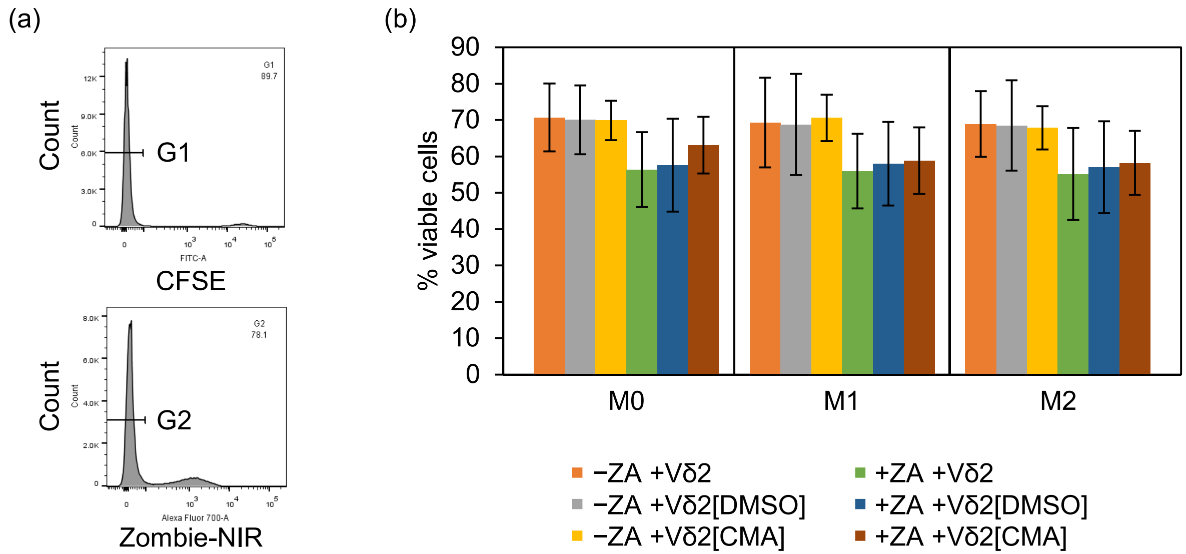

Supplementary Fig. 4: The effect of concanamycin A on the viability of Vδ2⁺ T cells. Different gates were applied to the data set shown in Fig. 4. **(a)** Representative flow cytometry plots from one of five donors showing the gating strategy used. $CFSE^{-}$ cells (i.e. $V\delta2^{+}$ T cells) were gated using G1. The percentage of Zombie-NIR^{low} cells (i.e. viable cells) within G1 was then determined using G2. **(b)** Means±SD for five donors.